Quantum Nature of Two-Dimensional Electron Gas Confinement at $LaAlO_3/SrTiO_3$ Interfaces

Karolina Janicka,[1] Julian P. Velev,[1,2] and Evgeny Y. Tsymbal[1]

[1]*Department of Physics, Nebraska Center for Materials and Nanoscience, University of Nebraska, Lincoln, Nebraska 68588, USA*
[2]*Department of Physics, Institute for Functional Nanomaterials, University of Puerto Rico, San Juan, Puerto Rico 00931, USA*

(Received 22 October 2008; published 10 March 2009)

We perform density functional calculations to understand the mechanism controlling the confinement width of the two-dimensional electron gas (2DEG) at $LaAlO_3/SrTiO_3$ interfaces. We find that the 2DEG confinement can be explained by the formation of metal induced gap states (MIGS) in the band gap of $SrTiO_3$. These states are formed as the result of quantum-mechanical tunneling of the charge created at the interface due to electronic reconstruction. The attenuation length of the MIGS into the insulator is controlled by the lowest-decay-rate evanescent states of $SrTiO_3$, as determined by its complex band structure. Our calculations predict that the 2DEG is confined in $SrTiO_3$ within about 1 nm at the interface.

DOI: 10.1103/PhysRevLett.102.106803 PACS numbers: 73.20.−r, 71.28.+d, 73.21.Cd, 73.40.Gk

Recent advances in thin-film deposition techniques, such as pulsed laser deposition and molecular beam epitaxy, have made it possible to fabricate oxide superlattices with atomically abrupt interfaces. At the interfaces of these heterostructures novel phases occur with interesting physical properties that are not present in the respective bulk constituents. In particular, it was found experimentally that a two-dimensional electron gas (2DEG) is formed at the LaO/TiO_2 interface between two common wide-gap insulating oxides $LaMO_3$ (M = Al, Ti) and $SrTiO_3$ making the interface conducting [1,2]. It was demonstrated that the 2DEG has high carrier mobility ($\sim 10\ cm^2/V\,s$) and electron density ($\sim 10^{14}\ cm^{-2}$) at room temperature, making it interesting for applications in all-oxide field-effect transistors [3]. It was also found that at low temperatures the 2DEG could become magnetic [4] or superconducting [5].

There are two explanations for the formation of the 2DEG at the LaO/TiO_2 interface of $LaMO_3/SrTiO_3$ (M = Al, Ti) heterostructures: electronic reconstruction and oxygen vacancies. Perovskite oxides exhibit a wide variety of valence states which can be described with the expression $A^{X+}B^{Y+}O_3{}^{2-}$, where $X + Y = 6$. In the [001] direction, the solid consists of alternating (001) planes of $A^{X+}O^{2-}$ and $B^{Y+}O_2{}^{2-}$ which can be charged. In particular, $LaAlO_3$ consists of alternating $(LaO)^+$ and $(AlO_2)^-$ charged planes and $SrTiO_3$ consists of alternating $(SrO)^0$ and $(TiO_2)^0$ neutral planes. This leads to the polar discontinuity at the interface, known as polar catastrophe, when $LaAlO_3$ is deposited on top of $SrTiO_3$. It was found that in semiconductors such a divergence of the electric potential can be avoided by atomic reconstruction at the interface [6,7]. In the case of LaO/TiO_2, however, mixed valence states of Ti allow for electronic reconstruction. The polar catastrophe can be avoided by transferring half of electron per two-dimensional unit cell from $LaAlO_3$ to $SrTiO_3$. These additional electrons occupy Ti $3d$ bands reducing its valence from Ti^{4+} (as in bulk $SrTiO_3$) toward Ti^{3+} and making the interface conducting [8].

Oxygen vacancies created during the growth of the oxide heterostructures play an important role in contributing to high sheet conductivities. This mechanism strongly depends on sample preparation conditions and is particularly important when small oxygen pressure is used during deposition [9–11]. There is, however, experimental evidence that under sufficiently high oxygen pressure electronic reconstruction is achieved and becomes the dominant effect [8].

First-principles calculations of $LaMO_3/SrTiO_3$ (M = Al, Ti) superlattices, based on density functional theory within the local density approximation (LDA) [12–14] and the LDA + U approximation [15–18], show the presence of n-type charge carriers (about $\frac{1}{2}$ electron on the interface Ti-$3d$ band) at the LaO/TiO_2 interface. This behavior is consistent with the electronic reconstruction mechanism, predicting metallicity of the LaO/TiO_2 interface. Some of the theoretical calculations address the mechanism of the 2DEG confinement formation. For example, Satpathy *et al.* [12] attribute the confinement of the 2DEG to a wedge-shaped potential well at the interface caused by the positive LaO charge density. Okamoto *et al.* [15] find the decay of the 2DEG charge density away from the interface which is explained by ionic screening due to lattice relaxations. However, none of the previous theoretical studies address the characteristic *confinement width* of the 2DEG and the physical mechanism controlling its magnitude.

The confinement width of a 2DEG is defined as the length across the interface over which the 2DEG is formed. Information about the confinement width is difficult to obtain experimentally. Most experimental setups require contacts to be constructed through the sample in order to reach the buried interface [1]. In this way the total current is detected but not the current distribution across the $SrTiO_3$ film. Very recently the cross section of the current distribution was mapped by scanning the cross-section with an atomic force microscope tip, and the 2DEG was found to be localized within a few nm at the interface [19]. The angle-dependent hard x-ray photoelectron spectros-

 © 2009 The American Physical Society

copy studies indicate that the 2DEG is indeed confined to a few unit cells at the interface [20]. However, the mechanism controlling the magnitude of the characteristic confinement width is not understood.

In this letter, we perform first-principles electronic structure calculations of $LaAlO_3/SrTiO_3$ superlattices with large unit cells and demonstrate that the confinement width of the 2DEG is determined by the metal induced gap states (MIGS) [21–23]. These states are formed within the insulating $SrTiO_3$ layer in the vicinity of the interface, as the result of quantum-mechanical tunneling of the charge created at the interface due to electronic reconstruction. The attenuation length of the MIGS into the insulator is controlled by the lowest-decay-rate evanescent states in $SrTiO_3$, as determined by the complex band structure of the insulator [21,24]. These states control the confinement width of the 2DEG at the $LaAlO_3/SrTiO_3$ interface. Our calculations predict that the attenuation length of the MIGS in $SrTiO_3$ is about 1 nm which determines the scale of the intrinsic confinement width of the 2DEG.

We obtain the atomic and electronic structure of $(LaAlO_3)_m/(SrTiO_3)_n$ superlattices (here m and n denote the numbers of monolayers of $LaAlO_3$ and $SrTiO_3$, respectively) using first-principles calculations based on density functional theory. To simulate large enough systems we use a plane-wave pseudopotential approach as implemented in the Vienna *ab initio* simulation package (VASP) [25]. The exchange-correlation potential is treated in the local density approximation. The in-plane lattice constant is fixed to the equilibrium value for cubic $SrTiO_3$ within LDA ($a = 3.87$ Å), while the c/a ratio is optimized for each supercell [26]. The ionic positions within this tetragonal cell are fully relaxed and demonstrate a substantial buckling of atoms consistent with the previously reported results [15].

Similar to the previous theoretical studies, we find that a 2DEG is formed at the LaO/TiO_2 interface in $(LaAlO_3)_m/(SrTiO_3)_n$ superlattices. The total amount of charge residing at the interface is $0.5e$ per lateral unit cell area, that corresponds to carrier density of about 3×10^{14} cm^{-2} consistent with experimental observations [3]. Our calculations for relatively small n demonstrate, however, a spurious distribution of the 2DEG due to artificial geometrical confinement within the $SrTiO_3$ layer. In order to fully resolve the attenuation of the charge density away from the interface, sufficiently large thickness of the $SrTiO_3$ layer is required. Therefore, we focus on $(LaAlO_3)_m/(SrTiO_3)_{23}$ supercell structures, with fixed thickness of $SrTiO_3$ corresponding to $n = 23$ and variable thickness of $LaAlO_3$ of $m = 1$, 3 and 5 monolayers.

Figure 1 shows the local density of states (DOS) on the TiO_2 planes located at different distance l (given in monolayers) from the LaO layer in $LaO/(SrTiO_3)_{23}$ superlattice ($m = 1$). A substantial band bending is seen resulting, in particular, in the change of the valence band maximum (VBM) and the conduction band minimum (CBM) as a function of l. This is due to the variation of the electrostatic

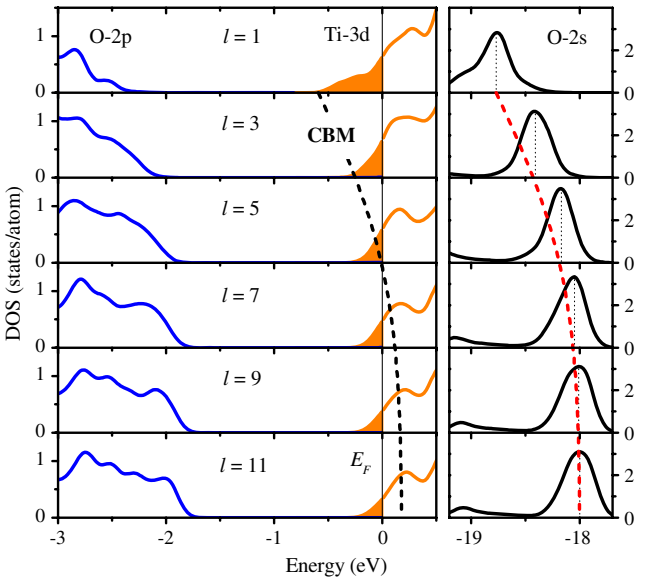

FIG. 1 (color online). Layer-resolved DOS on the TiO_2 planes in $LaO/(SrTiO_3)_{23}$ superlattice ($m = 1$). Index l denotes the TiO_2 monolayer position away from the LaO monolayer placed at $l = 0$. Left panels show the DOS in the vicinity of the Fermi energy (E_F) denoted by the vertical line. The shaded areas indicate the occupied states forming 2DEG. The dashed line demonstrates the variation of the conduction band minimum (CBM) in $SrTiO_3$. Right panels show the DOS of the O-2s states at energies around 18 eV below E_F. The potential variation is indicated by the dashed line.

potential which rigidly shifts the bands with respect of the Fermi energy (E_F). We obtain the site-dependent electrostatic potential using the corelike O-2s states shown in the right panels of Fig. 1. These states reveal a pronounced peak changing its position with l that we use for the analysis of the band bending. This allows us to find the variation of the CBM in $SrTiO_3$ as follows. We add the value $\Delta_g = 1.83$ eV corresponding to the calculated band gap for bulk $SrTiO_3$ to the VBM obtained for the TiO_2 monolayer at $l = 11$. This determines the CBM at this site, which appears to be approximately 0.18 eV above the Fermi energy. This is consistent with the experimental value of 0.25 ± 0.07 eV [27]. Then, we obtain the site variation of the CBM by adding the electrostatic potential difference from the shift of the core O-2s states. The result is shown by the dashed line in Fig. 1.

The important conclusion which follows from this analysis is the presence of the substantial valence charge occupying a classically forbidden region. This is seen from the relative position of the CBM with respect to the shaded area in Fig. 1 that indicates the amount of charge forming the 2DEG. For $l = 1$ and $l = 3$ almost all the charge resides in the region above the CBM. This is consistent with the classical picture of electrons confined in a potential well. However, for $l = 5$, 7, 9, and 11, we see that the charge occupies a classically forbidden region below the CBM. The physical mechanism responsible for this behav-

ior is quantum-mechanical tunneling under the potential barrier. The presence of the charge within the insulating band gap is the evidence for metal induced gap states (MIGS), a well-known quantum supplement of metal/insulator interfaces [21,23].

Figure 2 shows the charge distribution in the $SrTiO_3$ insulating layer, calculated from the integrated partial DOS on Ti sites, for $(LaAlO_3)_m/(SrTiO_3)_{23}$ structures with $m = 1$, 3, and 5. The total amount of the charge on Ti atoms is about $0.39e$. A fraction of this charge is confined on the first TiO_2 monolayer from where it decays exponentially in the bulk of $SrTiO_3$ with the characteristic attenuation length δ. We fit the charge distribution by $n \propto \exp(-z/\delta)$, where z is a distance from the interfacial TiO_2 monolayer, to obtain the attenuation length (see Fig. 2). [28] Not unexpectedly, we find that δ is almost independent of the number of $LaAlO_3$ monolayers and is equal to 1.03, 1.08, and 1.18 nm for $m = 1$, 3, and 5, respectively.

Figure 2 also shows the variation of the CBM within the $SrTiO_3$ layer obtained from the calculation described above. This may be regarded as an effective tunneling potential barrier for valence electrons residing at the interface. The Fermi level crossing separates classically allowed and classically forbidden regions in the insulator. The latter is indicated in Fig. 2 by the shaded area and contains about 0.42 of the total charge on Ti atoms. The presence of a charge in the classically forbidden region is the manifestation of the quantum nature of the 2DEG confinement. The classical electrostatic confinement potential is short ranged and extends only up to the second TiO_2 layer; however, the charge spills much further due to quantum tunneling which determines the confinement width of the 2DEG [29]. We note that insignificant amount of charge is induced in $LaAlO_3$. This is due to a much larger decay rate in the $LaAlO_3$ owing to the larger band gap and the fact that the Fermi level of the superlattice is closer to the middle of the $LaAlO_3$ band gap.

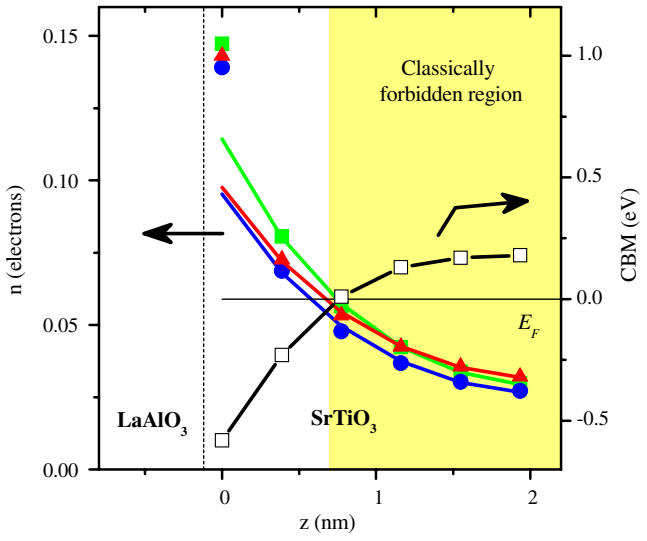

FIG. 2 (color online). Charge on Ti sites (solid symbols) for $(LaAlO_3)_m/(SrTiO_3)_{23}$ superlattices with $m = 1$ (squares), $m = 3$ (circles) and $m = 5$ (triangles), fitted charge distribution (solid lines), and the conduction band minimum (open squares) as a function of distance from the interface z. The interfacial TiO_2 monolayer is placed at $z = 0$ as a reference. The Fermi energy (E_F) is shown by a horizontal line and is related to the CBM plot only.

In order to obtain further insights into the electronic properties of the 2DEG, in Fig. 3(a) we have plotted $\mathbf{k}_\parallel$-resolved charge density of the 2DEG for the LaO/$(SrTiO_3)_{23}$ superlattice in the two-dimensional Brillouin zone, integrated in the range of energies from $E_F - 1$ eV to E_F, which contains the 2DEG. It is seen that the largest charge density is at the Γ point ($\mathbf{k}_\parallel = 0$). In the vicinity of the Γ point the charge distribution is reminiscent of a Fermi circle. This implies that free electron is a good starting approximation to investigate properties of the 2DEG. The spherical charge distribution for small $\mathbf{k}_\parallel$ is consistent with the band structure of the system (not shown) that reveals quadratic dispersion of the conduction bands close to the Γ point. By fitting these bands to a parabola we find the average effective mass $m^* \approx 9m_e$, which is consistent with the calculations performed for bulk $SrTiO_3$ [30]. Such a large value of the effective mass is due to the localized nature of the Ti-3d states resulting in low band dispersion and is detrimental to achieving high mobility of the 2DEG.

As we go away from the Γ point, the charge distribution pattern exhibits an outer region with lower charge density deviating from the circular shape. This is the consequence of the decay rate anisotropy in $SrTiO_3$. In order to reveal this anisotropy, we have calculated the complex band structure of bulk $SrTiO_3$. [31] Fig. 3(b) shows the lowest decay rate of the evanescent states as a function of $\mathbf{k}_\parallel$ evaluated at 0.2 eV below the CBM. In this energy range the lowest-decay-rate band has the Δ_5 symmetry. As seen, the states with the lowest decay rate form a cross pattern along the Γ-M directions in the two-dimensional Brillouin zone. In the area around the Γ point where the charge density is highest the decay rate is nearly constant and

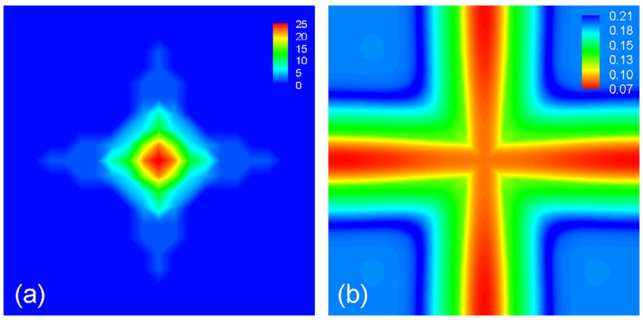

FIG. 3 (color online). $\mathbf{k}_\parallel$-resolved charge density of the LaO/$(SrTiO_3)_{23}$ superlattice (a) and the lowest decay rate of the evanescent states in bulk $SrTiO_3$ (b) within the two-dimensional Brillouin zone. The charge density is integrated in the energy range from $E_F - 1.0$ eV to E_F. The decay rate (in units of $2\pi/a$) is evaluated for bulk $SrTiO_3$ at 0.2 eV below the CBM.

the corresponding attenuation length is about $\delta \sim 0.8$ nm. This is in good agreement with the results of our supercell calculations. Thus, the complex band structure of bulk $SrTiO_3$ correctly estimates the attenuation length of the conduction charge density at the LaO/TiO_2 interface which confirms that the confinement of the 2DEG has a quantum nature and is governed by the formation of MIGS at the interface.

We, therefore, conclude that the $\mathbf{k}_\parallel$-dependent decay rate determines the shape of the charge density of the 2DEG in the two-dimensional Brillouin zone. Close to the zone center the decay rate is low and weakly dependent on $\mathbf{k}_\parallel$ producing a nearly spherical part of the charge density. Further away from the Γ point the decay rate sharply increases and exhibits strong anisotropy which is seen from the elongated contour of the charge density in the [100] and [010] directions.

We note that the well-known problem of LDA to underestimate the band gap does not affect significantly the predicted confinement width. The latter is determined by the conduction band bending due to the electrostatic potential that places the CBM at a certain position above the Fermi energy. In particular, the inclusion of electron correlations through LDA + U method [32,33] does not change significantly our results. This is consistent with the previous work [34]. Electron correlations affect the confinement through unequal occupation of the two spin channels which move slightly the charge center of mass further down in energy. Thus, the charge of the interface faces a slightly higher decay rate in the $SrTiO_3$ [31].

In conclusion, we find that the 2DEG at the LaO/TiO_2 interface of $LaAlO_3/SrTiO_3$ superlattices is confined in $SrTiO_3$ within about 1 nm from the interface. This 2DEG confinement is formed by the metal induced gap states (MIGS) in the insulator. The latter are the result of quantum-mechanical tunneling of the charge created at the interface due to electronic reconstruction. The MIGS are controlled by the complex band structure of the insulator through the decay rate of evanescent states. The predicted quantum nature of the 2DEGs at oxide interfaces needs to be taken into account when interpreting experimental data. We hope that our results will further stimulate the interest in elucidating properties of 2DEGs at oxide interfaces.

This work was supported by NRI/SRC, NSF MRSEC (NSF-DMR Grant No. 0820521) and the ONR (Grant No. N00014-07-1-1028). Work at UPR was supported by IFN (NSF Grant No. 0701525). Computations were performed at Research Computing Facility (UNL) and the Center for Nanophase Materials Sciences (ORNL).

[1] A. Ohtomo, D. A. Muller, J. L. Grazul, and H. Y. Hwang, Nature (London) **419**, 378 (2002).
[2] A. Ohtomo and H. Y. Hwang, Nature (London) **427**, 423 (2004).
[3] S. Thiel *et al.*, Science **313**, 1942 (2006).
[4] A. Brinkman *et al.*, Nature Mater. **6**, 493 (2007).
[5] N. Reyren *et al.*, Science **317**, 1196 (2007).
[6] G. A. Baraff, J. A. Appelbaum, and D. R. Hamann, Phys. Rev. Lett. **38**, 237 (1977).
[7] W. A. Harrison, E. A. Kraut, J. R. Waldrop, and R. W. Grant, Phys. Rev. B **18**, 4402 (1978).
[8] N. Nakagawa, H. Y. Hwang, and D. A. Muller, Nature Mater. **5**, 204 (2006).
[9] A. Kalabukhov *et al.*, Phys. Rev. B **75**, 121404(R) (2007).
[10] W. Siemons *et al.*, Phys. Rev. Lett. **98**, 196802 (2007).
[11] G. Herranz *et al.*, Phys. Rev. Lett. **98**, 216803 (2007).
[12] Z. S. Popovic and S. Satpathy, Phys. Rev. Lett. **94**, 176805 (2005).
[13] M. S. Park, S. H. Rhim, and A. J. Freeman, Phys. Rev. B **74**, 205416 (2006).
[14] J. Albina and C. Elsasser, Phys. Rev. B **76**, 165103 (2007).
[15] S. Okamoto, A. J. Millis, and N. A. Spaldin, Phys. Rev. Lett. **97**, 056802 (2006).
[16] R. Pentcheva and W. E. Pickett, Phys. Rev. B **74**, 035112 (2006); Phys. Rev. Lett. **99**, 016802 (2007).
[17] K. Janicka, J. P. Velev, and E. Y. Tsymbal, J. Appl. Phys. **103**, 07B508 (2008).
[18] J. Lee and A. A. Demkov, Phys. Rev. B **78**, 193104 (2008).
[19] M. Basletic *et al.*, Nature Mater. **7**, 621 (2008).
[20] M. Sing *et al.*, arXiv:0809.1917.
[21] V. Heine, Proc. Phys. Soc. London **81**, 300 (1963); Surf. Sci. **2**, 1 (1964); Phys. Rev. **138**, A1689 (1965).
[22] J. Tersoff, Phys. Rev. Lett. **52**, 465 (1984); **56**, 2755 (1986).
[23] G. Bordiera and C. Noguera, Surf. Sci. **251**, 457 (1991).
[24] P. Mavropoulos, N. Papanikolaou, and P. H. Dederichs, Phys. Rev. Lett. **85**, 1088 (2000).
[25] G. Kresse and J. Furthmüller, Phys. Rev. B **54**, 11 169 (1996); VASP (http://cms.mpi.univie.ac.at/vasp/).
[26] The energy cutoff for the plane-wave expansion was assumed to be 500 eV. Ionic relaxations were performed using k-points sampling with $8 \times 8 \times \max(1, 8/N)$ points in the irreducible Brillouin zone (N is number of unit cells perpendicular to the interface). Forces on each atom were converged to 10 meV/Å.
[27] K. Yoshimatsu, R. Yasuhara, H. Kumigashira, and M. Oshima, Phys. Rev. Lett. **101**, 026802 (2008).
[28] We note that the charge density in Fig. 2 is the superposition of the charge densities produced by two symmetric interfaces and therefore is doubled in the middle of the $SrTiO_3$ layer.
[29] The confinement width of a 2DEG is defined in our paper as the attenuation length of the exponentially decaying charge density (that is the distance from the interface where the charge density is dropped to $1/e$ of its value evaluated at the interface).
[30] W. Wunderlich, H. Ohta, and K. Koumoto, arXiv:cond-mat/0510013.
[31] J. P. Velev *et al.*, Phys. Rev. Lett. **95**, 216601 (2005).
[32] V. I. Anisimov, J. Zaanen, and O. K. Andersen, Phys. Rev. B **44**, 943 (1991); A. I. Liechtenstein, V. I. Anisimov, and J. Zaanen, *ibid.* **52**, R5467 (1995).
[33] LDA + U calculations were performed assuming $U =$ 5 eV and $J = 0.9$ eV on Ti $3d$ states.
[34] D. R. Hamman *et al.*, Phys. Rev. B **73**, 195403 (2006).